Coupled Nonlinear Microwave Oscillators
Electromagnetics Laboratory Report # 120
University of Colorado

Jonathan Dixon Zoya Popović

February 10, 1995

We begin with a model for the transistor, shown in Figure 1. This is the Curtice-Cubic model for a GaAs MESFET, with nonlinear equations for the drain-source current, the gate-drain diode, and the gate-source diode [1]. The equation for the drain-source current is

$$I_{ds} = \left(A_0 + A_1 v_1 + A_2 v_1^2 + A_3 v_1^3\right) \tanh\left(\gamma v_{ds}\right), \tag{1}$$

where

$$v_1 = v_{gs}\left[1 + \beta\left(v_{ds0} - v_{ds}\right)\right],$$

and the diodes are modeled by capacitors given by

$$C_d = C_{d0}\left(1 - \frac{v_{applied}}{v_{bi}}\right)^{-1/2} \tag{2}$$

in parallel with resistors given by

$$G_d = \frac{I_d}{V_d} = \frac{I_s}{V_d}\left(e^{V_d/nV_t} - 1\right). \tag{3}$$

We examined several oscillator topologies and chose to use the common-gate configuration, as shown in Figure 2. This choice was made because the common-gate is a very unstable layout, so it works well as an oscillator. The circuit was modeled by a system of differential/integral equations by using the Curtice-cubic transistor model and the standard linear models for the other circuit elements and applying Kirchoff's Current Law at each of the nodes of

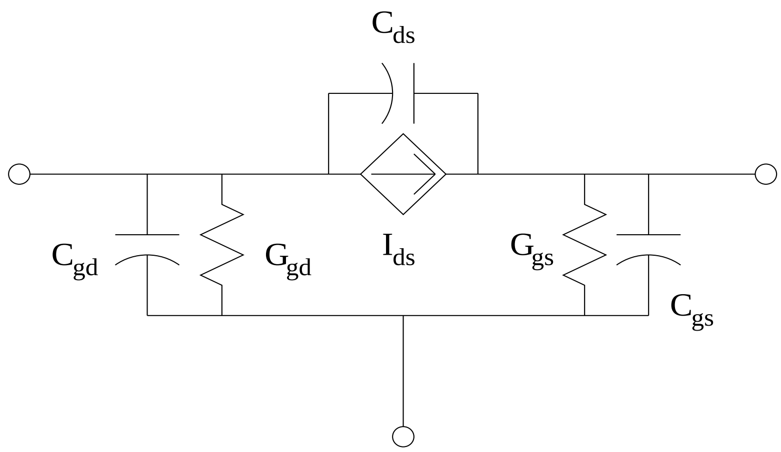

Figure 1: Transistor Model

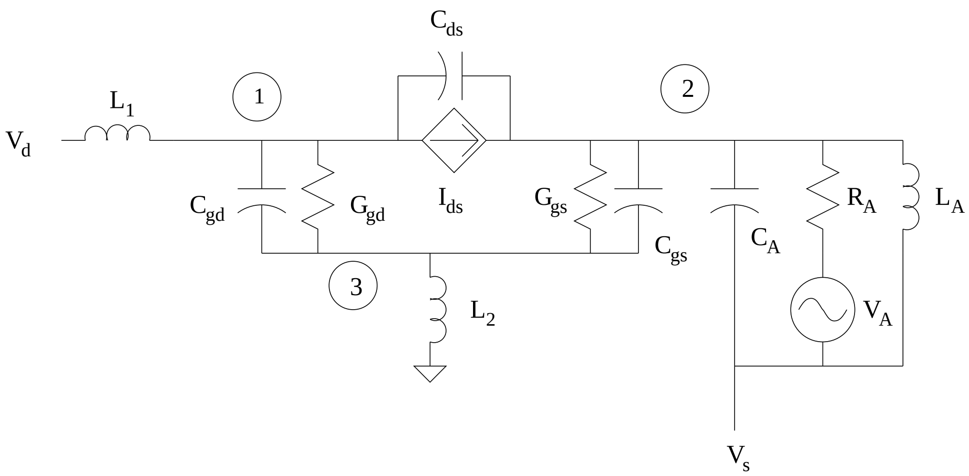

Figure 2: Common Gate Circuit

the circuit, yielding

$$\left.\begin{array}{rcl}
0 & = & \dfrac{1}{L_1}\displaystyle\int (v_1 - v_d)\,dt + C_{gd}\,(\dot{v}_1 - \dot{v}_3) + G_{gd}\,(v_1 - v_3) + \\
 & & \qquad C_{ds}\,(\dot{v}_1 - \dot{v}_2) + I_{ds} \\
0 & = & C_{ds}\,(\dot{v}_2 - \dot{v}_1) - I_{ds} + C_{gs}\,(\dot{v}_2 - \dot{v}_3) + G_{gs}\,(v_2 - v_3) + \\
 & & \qquad C_A\dot{v}_2 + \dfrac{v_2 - v_A - v_s}{R_A} + \dfrac{1}{L_A}\displaystyle\int (v_2 - v_s)\,dt \\
0 & = & \dfrac{1}{L_2}\displaystyle\int v_3 dt + C_{gd}\,(\dot{v}_3 - \dot{v}_1) + G_{gd}\,(v_3 - v_1) + C_{gs}\,(\dot{v}_3 - \dot{v}_2) + \\
 & & \qquad G_{gs}\,(v_3 - v_2)
\end{array}\right\} \qquad (4)$$

where dots over variables indicate derivatives with respect to time. The system is then differentiated again with respect to time. This makes the system a set of three coupled, second-order differential equations. When all the second-order terms are grouped together, we get

$$\left.\begin{array}{llcl}
\ddot{u}_1(C_{gd} + C_{ds}) & -\ddot{u}_2 C_{gd} & & = f \\
-\ddot{u}_1 C_{ds} & -\ddot{u}_2 C_{gs} & +\ddot{u}_3 C_A & = g \\
-\ddot{u}_1 C_{gd} & +\ddot{u}_2(C_{gd} + C_{gs}) & & = h
\end{array}\right\} \qquad (5)$$

where the u's are defined by

$$u_1 = v_1 - v_2$$
$$u_2 = v_3 - v_2$$
$$u_3 = v_2 - v_s$$

and f, g, and h are defined by

$$f = -\dot{I}_{ds} - \frac{1}{L_1}(u_1 + u_3 + v_s - v_d) - \left(\dot{C}_{gd} + G_{gd}\right)(\dot{u}_1 - \dot{u}_2) - \dot{G}_{gd}\,(u_1 - u_2)$$

$$g = \dot{I}_{ds} + \left(\dot{C}_{gs} + G_{gs}\right)\dot{u}_2 + \dot{G}_{gs}u_2 - \frac{\dot{u}_3 - \dot{v}_A}{R_A} - \frac{u_3}{L_A}$$

$$\begin{array}{rcl}
h & = & -\dfrac{1}{L_2}(u_2 + u_3 + v_s) - \left(\dot{C}_{gd} + G_{gd}\right)(\dot{u}_2 - \dot{u}_1) - \dot{G}_{gd}\,(u_2 - u_1) - \\
 & & \qquad \left(\dot{C}_{gs} + G_{gs}\right)\dot{u}_2 - \dot{G}_{gd}u_2
\end{array}$$

The change of variables from v to u is necessary to avoid singularities when solving for the second-order terms. Using $u_4 = \dot{u}_1$, $u_5 = \dot{u}_2$, and $u_6 = \dot{u}_3$ and solving analytically for the first derivatives we get

$$\left.\begin{array}{rcl}
\dot{u}_1 & = & u_4 \\
\dot{u}_2 & = & u_5 \\
\dot{u}_3 & = & u_6 \\
\dot{u}_4 & = & \dfrac{k_1\,(f + C_{gd}h')}{k_2} \\
\dot{u}_5 & = & \dfrac{C_{gd}}{k_2}(f + C_{gd}h') + h' \\
\dot{u}_6 & = & \dfrac{1}{C_A}(f + g + h)
\end{array}\right\} \qquad (6)$$

where

$$k_1 = C_{gd} + C_{gs}$$
$$k_2 = C_{gs}C_{gd} + C_{ds}C_{gd} + C_{gs}C_{ds}$$
$$h' = \frac{h}{k_1}$$

Since all of these quantities use the values of the non-linear capacitances and conductances, and the derivatives of the capacitances, conductances, and the drain-source current, it is necessary to have a means to calculate them. Using equations 1-3, modified to better model the effects of forward biasing the diode j
uctions, we have

$$C_{gs,gd} = \begin{cases} C_{gs0,gd0}\left(1 - \frac{v_{gs,gd}}{v_{bi}}\right)^{-1/2} & v_{gs,gd} < v_{bi}\left(1 - \frac{1}{1000^2}\right) \\ 1000C_{gs0,gd0} & \text{otherwise} \end{cases} \tag{7}$$

$$\dot{C}_{gs,gd} = \begin{cases} \frac{C_{gs0,gd0}}{2v_{bi}}\left(1 - \frac{v_{gs,gd}}{v_{bi}}\right)^{-3/2}\dot{v}_{gs,gd} & v_{gs,gd} < v_{bi}\left(1 - \frac{1}{1000^2}\right) \\ 0 & \text{otherwise} \end{cases} \tag{8}$$

$$G_{gs,gd} = \begin{cases} \frac{I_s}{v_{gs,gd}}\left(e^{v_{gs,gd}/nV_t} - 1\right) & v_{gs,gd} \neq 0 \\ \frac{I_s}{nV_t} & v_{gs,gd} = 0 \end{cases} \tag{9}$$

$$\dot{G}_{gs,gd} = \begin{cases} \frac{I_s\dot{v}_{gs,gd}}{nV_t v_{gs,gd}}e^{v_{gs,gd}/nV_t} - \frac{I_s\dot{v}_{gs,gd}}{v^2_{gs,gd}}\left(e^{v_{gs,gd}/nV_t} - 1\right) & v_{gs,gd} \neq 0 \\ \frac{I_s}{2nV_t^2}\dot{v}_{gs,gd} & v_{gs,gd} = 0 \end{cases} \tag{10}$$

and

$$\begin{aligned} \dot{I}_{ds} &= \tanh(\gamma v_d s)(A_1 + 2A_2v_1 + 3A_3v_1^2)\dot{v}_1 + \\ &\qquad \gamma(A_0 + A_1v_1 + A_2v_2^2 + A_3v_3^3)\operatorname{sech}^2(\gamma v_{ds})\,\dot{v}_{ds} \end{aligned} \tag{11}$$

where v_1 is defined as in (1) and

$$\dot{v}_1 = \dot{v}_{gs}\left[1 + \beta(v_{ds0} - v_{ds})\right] - v_{gs}\beta\dot{v}_{ds}$$

These equations were implemented in Fortran 77, using a Fourth-Order Runge-Kutta numeric integration routine, on an HP 9000/720, using the f77 compiler for HP-UX 9.0 with level 3 optimization.

For initial testing and verification of the numeric model, we chose to use typical device parameters based on values for FETs from M/A–COM. The values we used were

$$
\begin{aligned}
C_{gs0} &= 12.0\,\mathrm{nF} \\
C_{gd0} &= 0.3\,\mathrm{nF} \\
v_{bi} &= 0.8\ \mathrm{V} \\
\gamma &= 2.0\ \mathrm{V}^{-1} \\
A_0 &= 1.8\ \mathrm{V}^{-1} \\
A_1 &= 0.67\,\mathrm{V}^{-1} \\
A_2 &= -0.58\ \mathrm{V}^{-1} \\
A_3 &= -0.23\ \mathrm{V}^{-1} \\
\beta &= 0.05\ \mathrm{V}^{-1} \\
v_{ds0} &= 8.0\ \mathrm{V} \\
C_{ds} &= 5.0\,\mathrm{nF} \\
I_s &= 1.0 \times 10^{-7}\ \mathrm{A} \\
nv_t &= 0.026\ \mathrm{V}
\end{aligned}
$$

Running this through the program gave

$$
\begin{aligned}
R_A &= 50\ \Omega \\
C_A &= 0.01\,\mathrm{nF} \\
L_A &= 0.5\,\mathrm{nH} \\
L_1 &= 2.0\,\mathrm{nH} \\
L_2 &= 0.3\,\mathrm{nH} \\
v_d &= 3.0\ \mathrm{V} \\
v_s &= 1.0\ \mathrm{V}
\end{aligned}
$$

for 500 nsec with a 1 psec timestep, we get a five-cycle oscillation. The output voltage of this circuit (the voltage across the antenna resistance) can be seen in Figure 3. By cutting off the first 200 nsec of data (to allow for the transients to die out) and then plotting the derivative of the output voltage against the output voltage, we can clearly see the five-cycle oscillation, shown in Figure 4. This is significant because it strongly suggests the presence of chaotic behavior at some point in the parameter space, inasmuch as it resembles the work of Li and Yorke [2]. In fact, with $I_s = 0$ A and $v_s = 0.8$ V we get results, shown in Figure 5 and Figure 6, which because of the fractal appearance of their phase-space representation and lack of apparent periodicity, appear to be chaotic.

After this test showed that the program was running satisfactorally, a more realistic test of the program was desired. For this, parameters based on [3] (with estimations on the unknown parameters) were used in simulations. The values used for this were

$$C_{gs0} = 0.425 \times 10^{-3}\,\mathrm{nF}$$

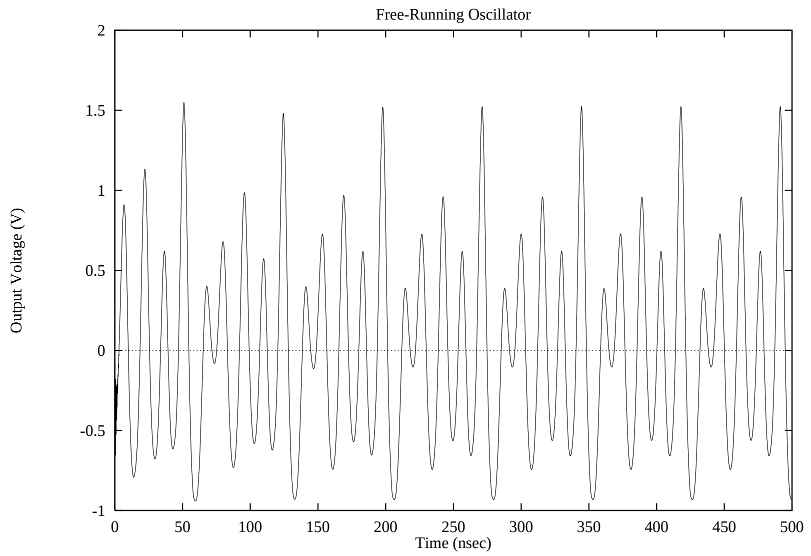

Figure 3: Five-Cycle Oscillation – Time Domain

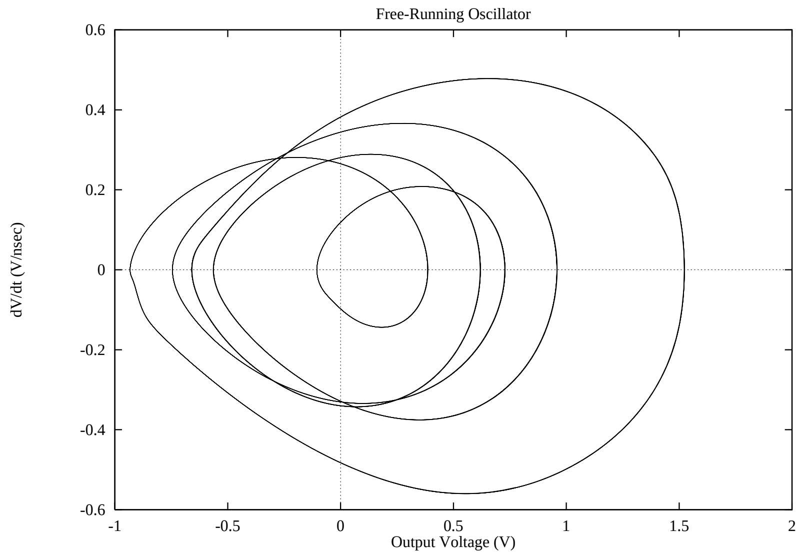

Figure 4: Five-Cycle Oscillation – Phase Space

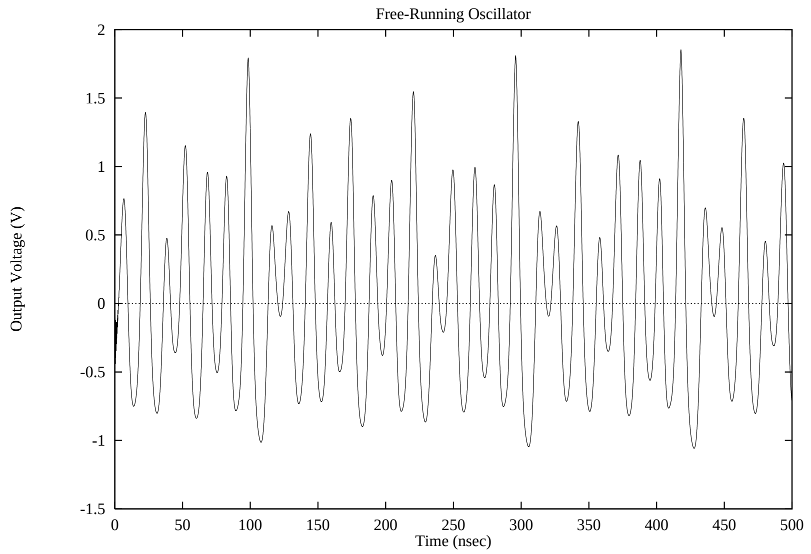

Figure 5: Apparent Chaotic Behavior – Time Domain

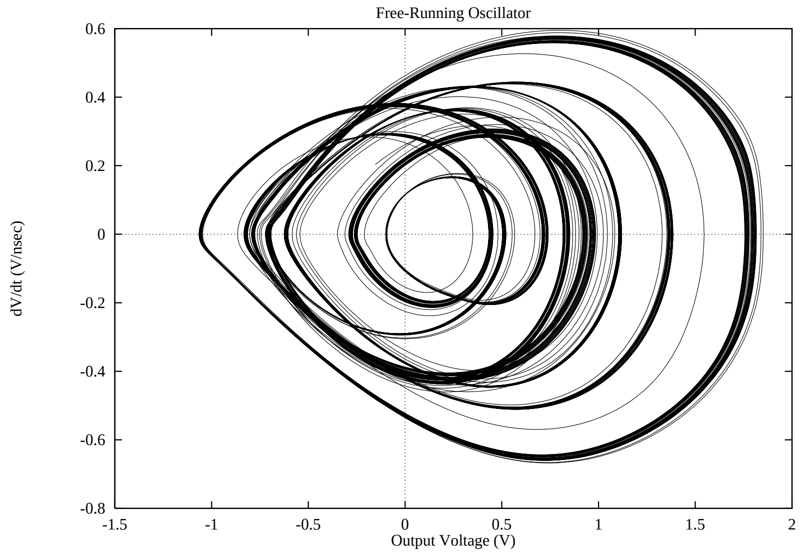

Figure 6: Apparent Chaotic Behavior – Phase Space ($500 < t < 5000$ nsec)

$$
\begin{aligned}
C_{gd0} &= 0.086 \times 10^{-3}\,\mathrm{nF} \\
v_{bi} &= 0.8\,\mathrm{V} \\
\gamma &= 2.0\,\mathrm{V}^{-1} \\
A_0 &= 1.8\,\mathrm{V}^{-1} \\
A_1 &= 0.67\,\mathrm{V}^{-1} \\
A_2 &= -0.58\,\mathrm{V}^{-1} \\
A_3 &= -0.23\,\mathrm{V}^{-1} \\
\beta &= 0.05\,\mathrm{V}^{-1} \\
v_{ds0} &= 8.0\,\mathrm{V} \\
C_{ds} &= 0.378 \times 10^{-3}\,\mathrm{nF} \\
I_s &= 1.0 \times 10^{-7}\,\mathrm{A} \\
nv_t &= 0.026\,\mathrm{V} \\
R_A &= 50\,\Omega \\
C_A &= 0.1\,\mathrm{nF} \\
L_A &= 0.2\,\mathrm{nH} \\
L_1 &= 0.2\,\mathrm{nH} \\
L_2 &= 0.3\,\mathrm{nH} \\
v_d &= 3.0\,\mathrm{V} \\
v_s &= 0.7\,\mathrm{V}
\end{aligned}
$$

This resulted in an oscillation at about 12.5 GHz. The time domain response can be seen in Figure 7 and the phase space response is in Figure 8. While this is a very low-power oscillation, it at least shows that this model can generate high-frequency oscillations with proper loading circuitry and FETs.

The next step was to generalize the model. Using the layout in Figure 9, and the variables

$$u_1 = v_1 - v_2 = v_{ds},$$

$$u_2 = v_3 - v_2 = v_{gs},$$

and

$$u_3 = v_2,$$

together with Kirchoff's Current Law at each node we wind up with

$$
\left.
\begin{aligned}
I_{in1} &= C_{gd}(\dot{u}_1 - \dot{u}_2) + G_{gd}(u_1 - u_2) + I_{ds} + C_{ds}\dot{u}_1 \\
0 &= I_{in2} + I_{ds} + C_{ds}\dot{u}_1 + C_{gs}\dot{u}_2 + G_{gs}u_2 \\
I_{in3} &= C_{gd}(\dot{u}_2 - \dot{u}_1) + G_{gd}(u_2 - u_1) + C_{gs}\dot{u}_2 + G_{gs}u_2
\end{aligned}
\right\} \tag{12}
$$

Since $u_3$no longer appears explicitly in these equations (although it affects the input currents), this is essentially a system of three equations with two unknowns. By first differentiating the system with respect to time and then arbitrarily choosing the first and third equations from the system, we get

$$
\left.
\begin{aligned}
\ddot{u}_1\,(C_{gd} + C_{ds}) \quad -\ddot{u}_2 C_{gd} &= g \\
-\ddot{u}_1 C_{gd} \quad +\ddot{u}_2\,(C_{gd} + C_{gs}) &= h
\end{aligned}
\right\} \tag{13}
$$

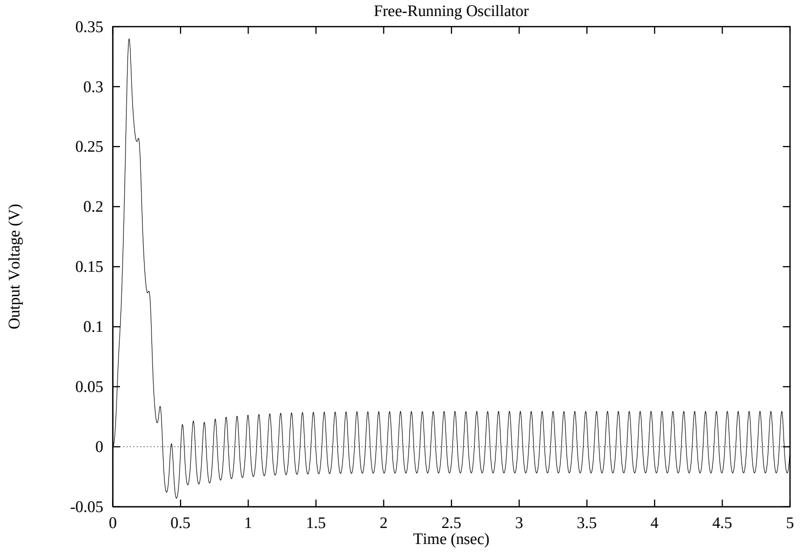

Figure 7: High Frequency Oscillation – Time Domain

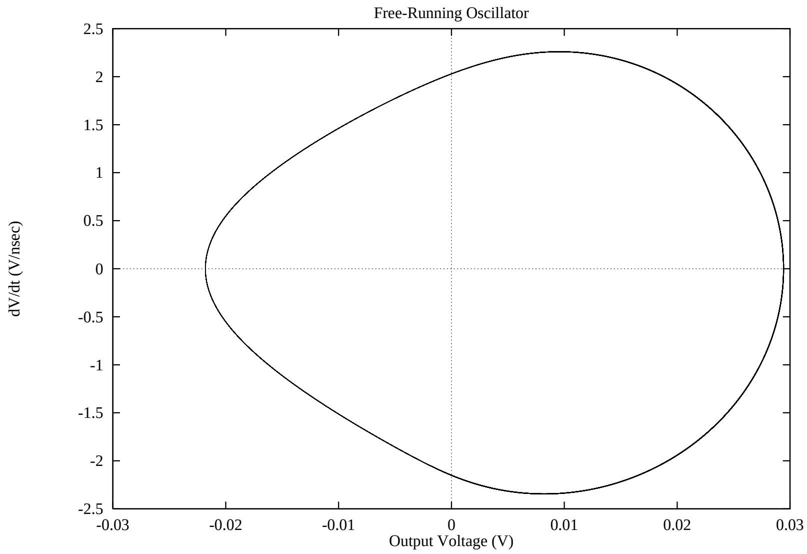

Figure 8: High Frequency Oscillation – Phase Space ($5 < t < 25$ nsec)

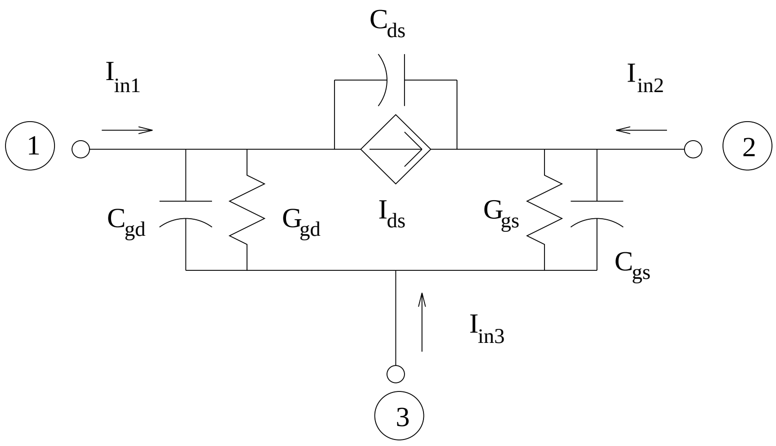

Figure 9: Transistor Model

where

$$g = \dot{I}_{in1} - (\dot{u}_1 - \dot{u}_2)\left(\dot{C}_{gd} + G_{gd}\right) - \dot{G}_{gd}(u_1 - u_2) - \dot{I}_{ds}$$

and

$$\begin{aligned} h &= \dot{I}_{in3} - (\dot{u}_2 - \dot{u}_1)\left(\dot{C}_{gd} + G_{gd}\right) - \dot{G}_{gd}(u_2 - u_1) - \\ &\quad \dot{u}_2\left(\dot{C}_{gs} + G_{gs}\right) - u_2\dot{G}_{gs} \end{aligned}$$

By subtracting the first and third equations from the second equation in (12) we get the constraint

$$\dot{I}_{in1} + \dot{I}_{in2} + \dot{I}_{in3} = 0 \tag{14}$$

which must be satisfied in order for the system of equations to be consistent.

In a similar manner to that used in the derivation of (5), we transform (13) into

$$\left.\begin{aligned} \dot{u}_1 &= u_3 \\ \dot{u}_2 &= u_4 \\ \dot{u}_3 &= g' + \frac{h'}{k_1} \\ \dot{u}_4 &= g'k_2 + h'\left(1 + \frac{k_2}{k_1}\right) \end{aligned}\right\} \tag{15}$$

where

$$k_1 = 1 + \frac{C_{ds}}{C_{gd}} - k_2$$

$$k_2 = \frac{C_{gd}}{C_{gs} + C_{gd}}$$

$$g' = \frac{gC_{gd}}{k_1}$$

$$h' = \frac{h}{C_{gd} + C_{gs}}$$

We then calculate $\dot{I}_{in1}$ and $\dot{I}_{in3}$ using u_1,u_2,u_3, $\dot{u}_1$,$\dot{u}_2$, and $\dot{u}_3$ and we calculate $\dot{I}_{in2}$ using (14). Once all of these values are known, we solve for u_3 and $\dot{u}_3$. The exact process used to get these will depend upon the particular circuitry attatched to the port, although more circuits will require the use of some form of numerical integration. An example of the equations for u_3 and $\dot{u}_3$ one gets by attaching a parallel RLC circuit (such as is on the output of the previous topology) is

$$\ddot{u}_3 = \frac{1}{C_A}\left(-\dot{I}_{in2} + \frac{\dot{v}_A - \dot{u}_3}{R_A} + \frac{v_s - u_3}{L_A}\right) \tag{16}$$

Finally, (15) is solved using Fourth-Order Runge-Kutta.

References

[1] W. R. Curtice and M. Ettenberg, "A nonlinear GaAs FET model for use in the design of output circuits for power amplifiers," *IEEE Trans. Microwave Theory Tech.* vol. 33, pp. 1383–1394 1985.

[2] Tien-Yien Li and James A. Yorke, "Period three implies chaos," *Amer Math Monthly* pp. 985–992 1982.

[3] Chien-Chang Huang and Tah-Hsiung Chu, "Analysis of MESFET injection-locked oscillators in fundamental mode of operation," *IEEE Trans. Microwave Theory Tech.* vol. 42, pp. 1851–1857 1994.